Supporting Information for

Active Site Metal Occupancy and Cyclic di-GMP Phosphodiesterase Activity of *Thermotoga maritima* HD-GYP

Kyle D. Miner, and Donald M. Kurtz, Jr.*

Department of Chemistry, University of Texas at San Antonio, San Antonio, Texas 78249, United States

This work was supported by National Institutes of Health Grants R01 GM040388 to D.M.K.

*Contact Information of Corresponding Author

E-mail: donald.kurtz@utsa.edu

Molecular Dynamics Simulations

Molecular dynamics simulations were carried out to generate a structural model of TM0186 containing a dimetal site analogous to that in Bd1817 (Figure 1B) in a protein framework modeled on PmGH. The coordinates for the TM0186 HD-GYP domain were from a structure homology model generated using the SWISS-MODEL web server (http://swissmodel.expasy.org/) with the TM0186 amino acid sequence as input and the PmGH trimetal protein structure as template. The HD-GYP domain model returned by the SWISS-MODEL web server included residues 149-341 of the TM0186 amino acid sequence without metal, solvent, or other exogenous atoms. The program visual molecular dynamics (VMD)[1] was employed to prepare structure files and run the simulations. Using the STAMP[2] structural alignment tool, an RMSD overlay was then obtained of the PmGH crystal structure (PDB ID 4MCW) and the TM0186 structural model to determine the optimum coordinates of the three metals in the TM0186 model. The exogenous succinate and imidazole ligands in the PmGH 4MCW structure were omitted when generating the TM0186 triiron model and M1,M2 and M2,M3 bridging solvent positions were inserted from the PmGH crystal structure. An overlay of the triiron site in the TM0186 model and the PmGH crystal structure is shown in Figure S9. For the molecular dynamics simulations a generic divalent closed shell metal ion (identified as ZN2 in charmm27) was placed in the PDB coordinates file of the TM0186 model at the M1 and M3 positions, and a water molecule was placed at the M2 position. Water molecules were added at positions corresponding to the metal ligating atoms of exogenous succinate and imidazole from the PmGH crystal structure. The protein was placed in a solvation box with explicit water molecules extending 15 Å beyond the protein in x, y, and z directions using the solvation plugin of VMD. M1 and M3 ligand bonds were constrained to those analogous to the dimetal site in

Bd1817 as follows. Protein ligating atoms in the starting TM0186 model were constrained at a distance of 2.1 Å and a spring constant of 250 kcal/mol/Å^2 for M1 to NE2 of H234, H260, H261, and OD1 of D206, or M3 to NE2 of H173, H205, OD1 of D289, and OD2 of D206. No metal-E169 distance or bonding constraints were applied. A bridging interaction was defined between M1, the water substituted at the M2 position and M3, in which the metal-oxygen distances were constrained to 1.8 Å with a spring constant of 250 kcal/mol/Å^2, and the M1-oxygen-M3 angle was constrained to 125 degrees (based on the average M1-(solvent bridge)-M2 and M2-(solvent bridge)-M3 angles in the PmGH 4MCW coordinates) and a spring constant of 35 kcal/mol/rad^2. This solvated protein system was used as input for the program Nanoscale Molecular Dynamics (NAMD)[3] using VMD's NAMD GUI. The minimization and molecular dynamic simulation were carried out in steps using the variable pressure, variable energy NVT ensemble and standard charmm27 force field for 0.1 nsec at 0 K and 0.5 nsec at 298K respectively using a 1fs step size. The final positioning of the atoms in the dimetal site of the TM0186 model is shown in Figure 7B. An overlay of the starting triiron and final diiron TM0186 protein backbones models is shown in Figure S10.

An analogous trimetal-to-dimetal molecular dynamics simulation was performed for the PmGH crystal structure (PDB ID 4MCW), which contains a non-crystallographically symmetrical protein dimer with a triiron site in each subunit. Metal/ligand substitutions and initial constraints analogous to those described above for the TM0186 simulation were applied to both subunits. The simulation returned a protein dimer model in which the dimetal site in one subunit had E185 monodentately coordinated to M2 (M2-OE2 distance = 2.0 Å), and the dimetal site in the other subunit had a non-coordinating E185. Depictions of these PmGH "E185 on" and

"E185 off" dimetal site structural models and a protein backbone overlay of the PmGH triiron crystal structure (4MCW) and PmGH dimetal model are shown in Figure S11.

```
                          *   *
TM0186    MLSEYR--DMETHRHTERVGWLSGRIAEEMGMSEVFVTEIQFAAP--------LHDIGKI
PmGH      HATKFK--DPETQNHIIRVGLYCEILAREAGLDEEDVELVKLAAP--------MHDIGKV
Bd1817    AVMNIENTDKTISHHGVTVSTLSIALAQKLGITDPKKTQLLTLGA-------LLHDYGHH
PA4781    TLGDLR--DNPRSRHLPRIERYVRLLAEHLAAQRAFADELTPEAVDLLSKSALLHDIGKV

TM0186    GIPDRILLKPGILTPEEFEIMKQHTTIGFRILSRSN------SPILQLGAEIALTHHERW
PmGH      GIPDRVLLKPGKLNDEEWEIMKKHTIYGYEILKGGD------SRLLQIAADIAIEHHERW
Bd1817    HSPLNLNQPLDSMSPEDLALWKKHPIEGAQKVQDKK-------HFDQTVINIIGQHEETI
PA4781    AVPDRVLLNPGQLDAADTALLQGHTRAGRDALASAERRLGQPSGFLRFARQIAYSHHERW

                                    *
TM0186    DGSGYPRGLKEREIPISGLIVAVADSFDAMVSRRPYKNPKPLEEAFREIESLSGKLYSPE
PmGH      DGTGYPFGKKGEEISIYGRMTSISDVFDALTSDRPYKKAWDMDRTVRFFKEQKGKHFDPF
Bd1817    NGTG-PKGLREKDMDPLAVLVSSANAMDRLITFEGVPKAEAAKKLMIDHVGKHPLQHIQH
PA4781    DGRGFPEGLAGERIPLAARIVALADRYDELTSRHAYRPPLAHAEAVLLIQAGAGSEFDPR
```

Figure S1. Amino acid sequence alignment of the HD-GYP domains of *Thermotoga maritima* TM0186, *Persephonella marina* PmGH, and *Bdellovibrio bacteriovorus* Bd1817. Highlight color coding: Structurally verified (PmGH, Bd1817, and PA4781) or putative (TM0186) metal ligand residues (yellow) and GYP motif (pink). Stars indicate TM0186 residues E169, H173, and D289, which were changed individually to A in this study.

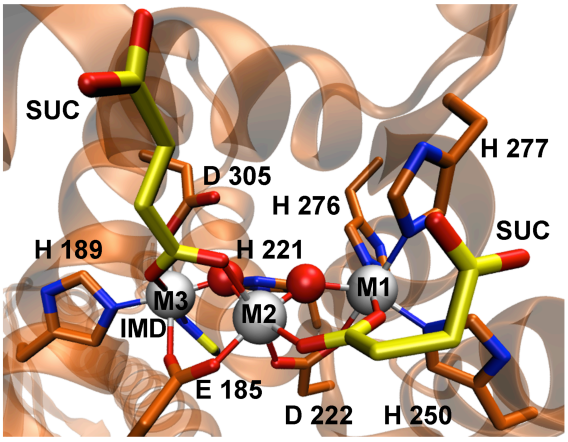

Figure S2. The triiron site in the PmGH HD-GYP crystal structure (PDB ID 4MCW) depicted as in Figure 1A but including exogenous succinate and imidazole iron ligands. Iron atoms are represented as grey spheres and bridging solvent ligands as red spheres. Protein backbone and side chains are represented in orange. Exogenous succinate (SUC) and imidazole (IMD) ligands are shown in yellow.

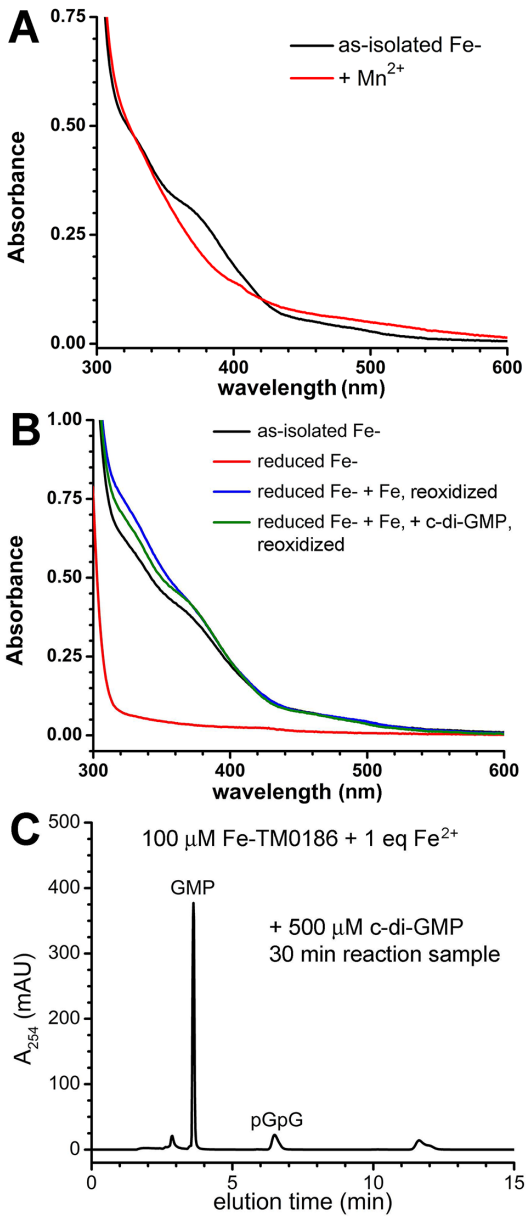

Figure S3. UV-visible spectra of (A) 50 µM Fe-TM0186 as-isolated in the absence (black) or presence (red) of 10 mM manganous chloride. (B) Anaerobic UV-visible absorption spectra of 50 uM Fe-TM0186 in the as-isolated (black), reduced (red), re-oxidation with air after addition of +1eq Fe and incubation at 37 ^{0}C (blue) with addition of +1eq Fe and incubation at 37 ^{0}C then addition of +5eq c-di-GMP for 30 min (green). (C) HPLC chromatogram for c-di-GMP PDE activity of 100 uM reduced Fe-TM0186 + 1eq ferrous ammonium sulfate at 37 °C, 30 min refers to the time the reaction mixture was sampled after addition of 5eq c-di-GMP.

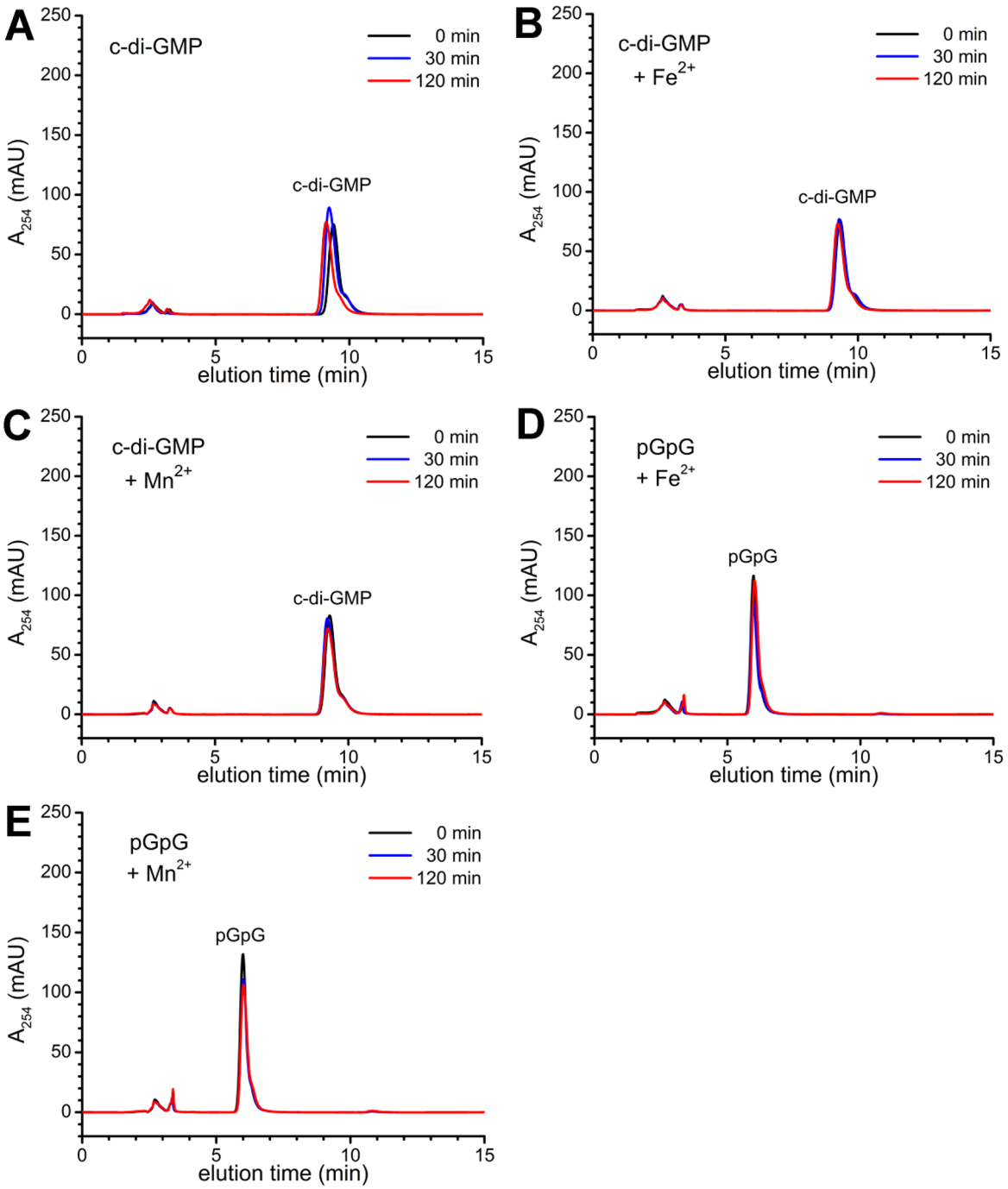

Figure S4. HPLC chromatograms for c-di-GMP incubated at 37 °C in the (A) absence or presence of either (B) 80 μM ferrous ammonium sulfate ($+Fe^{2+}$) or (C) 10 mM manganous chloride ($+Mn^{2+}$) or pGpG incubated at 37 °C in the presence of either (D) 80 μM ferrous ammonium sulfate ($+Fe^{2+}$) or (E) 10 mM manganous chloride ($+Mn^{2+}$) and sampled at the indicated times.

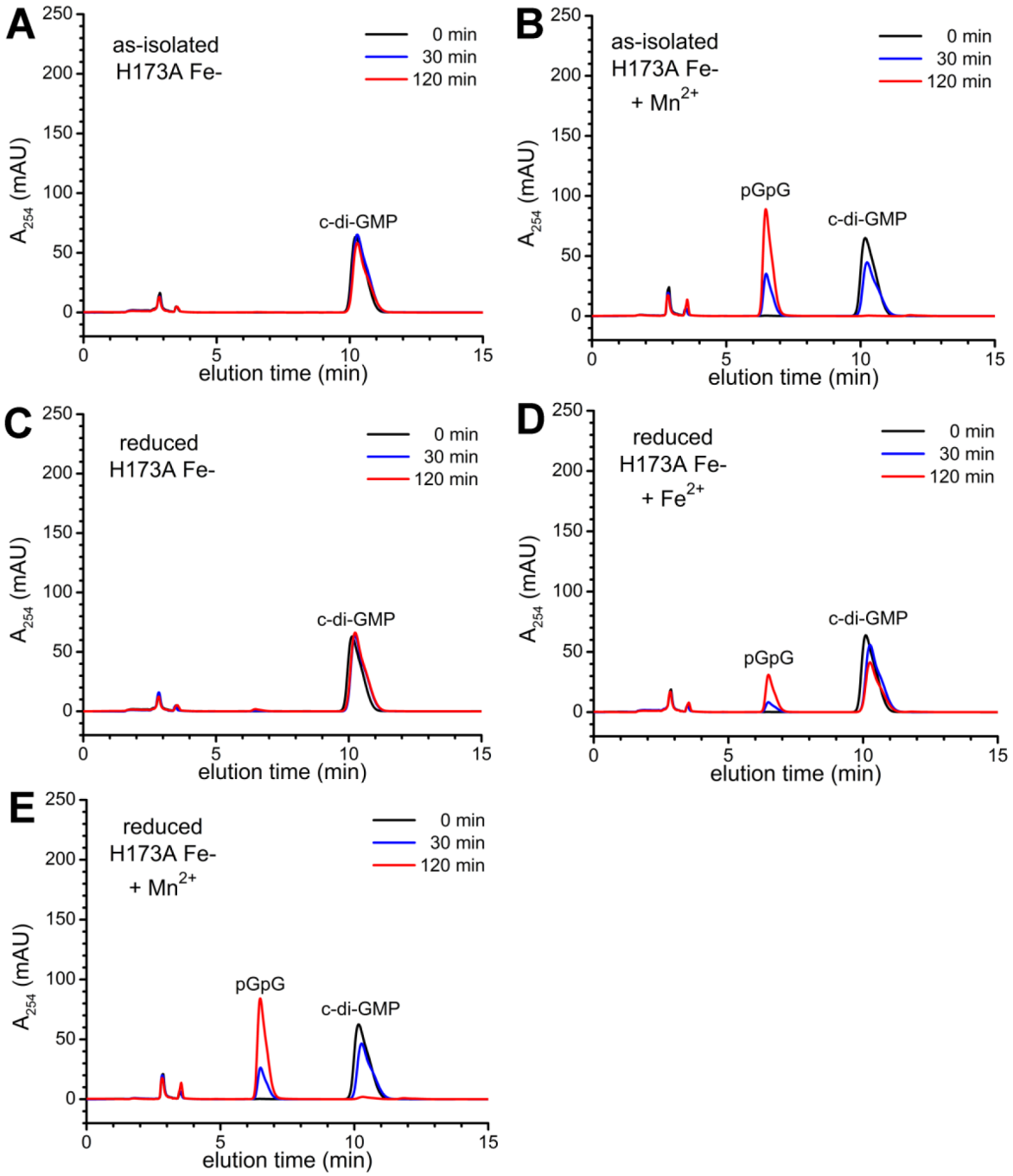

Figure S5. HPLC chromatograms for c-di-GMP PDE activities of H173A Fe-TM0186 (A) as-isolated (B) as-isolated and pre-incubated with 10 mM manganous chloride ($+Mn^{2+}$) (C) reduced, (D) reduced and pre-incubated with 80 μM ferrous ammonium sulfate ($+Fe^{2+}$), or (E) reduced and preincubated with 10 mM manganous chloride ($+Mn^{2+}$), and sampled at the indicated times following addition of c-di-GMP.

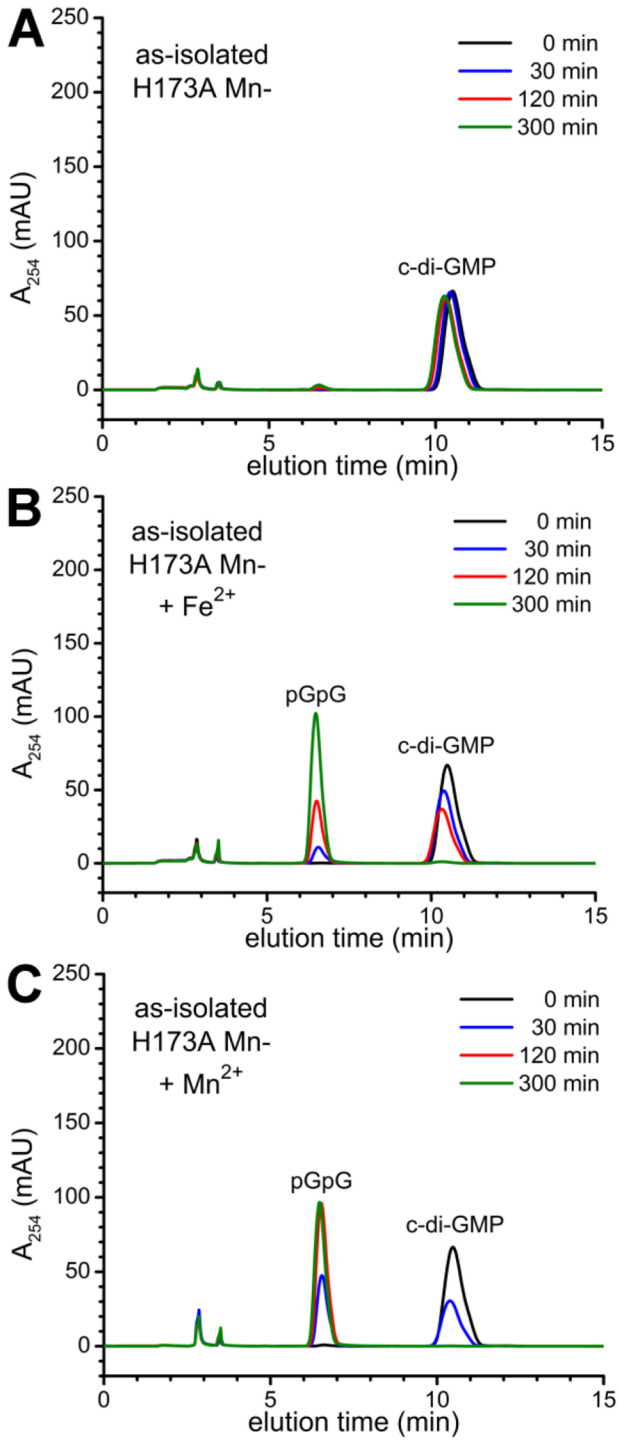

Figure S6. HPLC chromatograms for c-di-GMP PDE activities of as-isolated H173A Mn-TM0186 anaerobically incubated with (A) no added metal, (B) 80 uM ferrous ammonium sulfate, or (C) 10 mM manganous chloride, and sampled at the indicated times following addition of c-di-GMP.

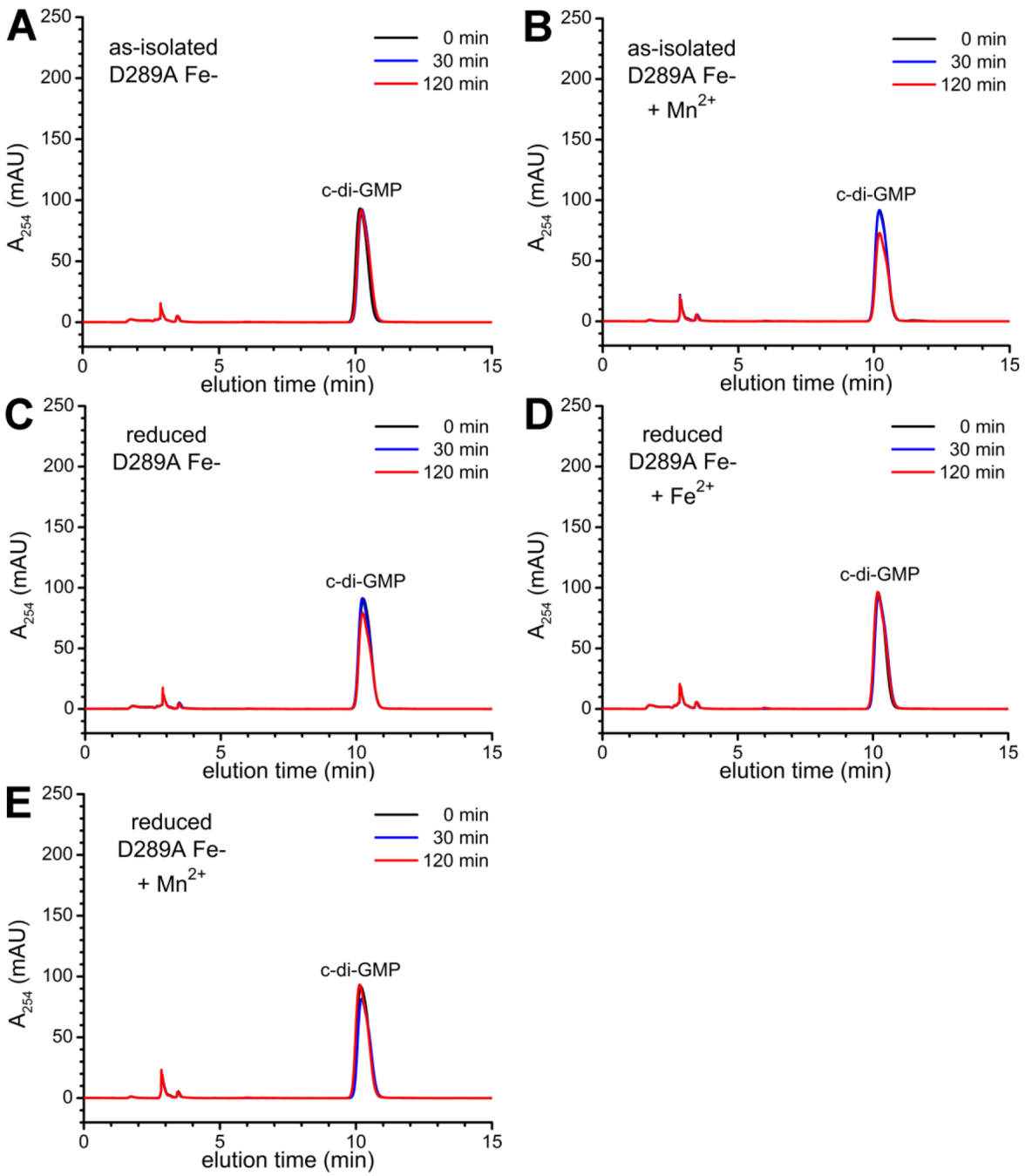

Figure S7. HPLC chromatograms for c-di-GMP PDE activities of D289A Fe-TM0186 (A) as-isolated (B) as-isolated and pre-incubated with 10 mM manganous chloride ($+Mn^{2+}$) (C) reduced, (D) reduced and pre-incubated with 80 μM ferrous ammonium sulfate ($+Fe^{2+}$), or (E) reduced and preincubated with 10 mM manganous chloride ($+Mn^{2+}$), and sampled at the indicated times following addition of c-di-GMP.

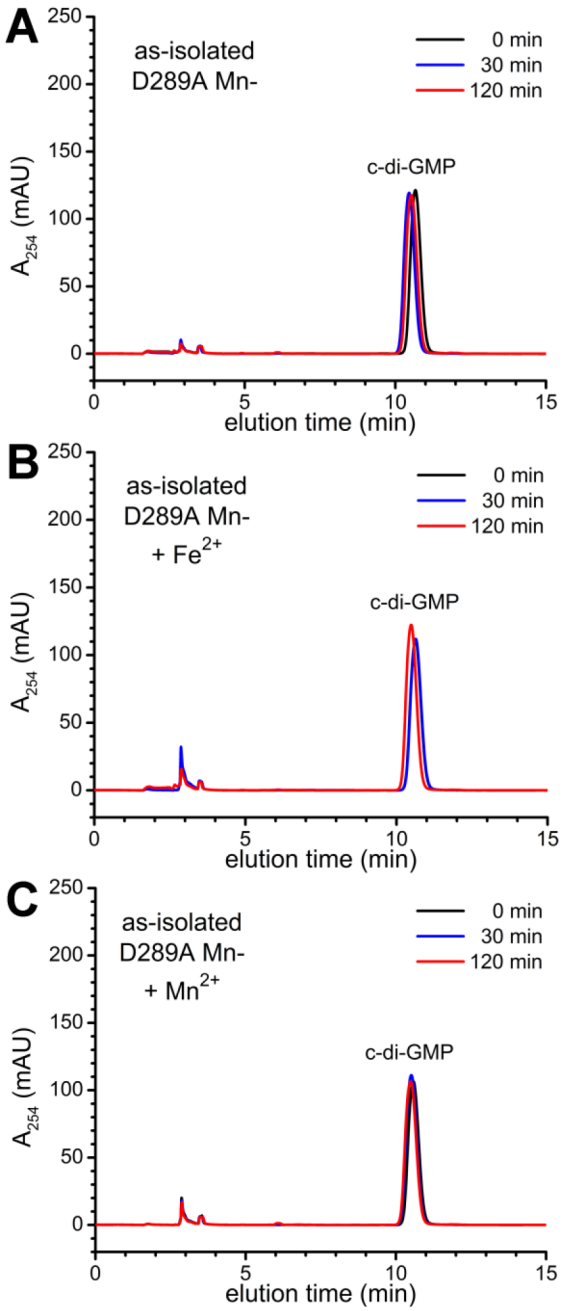

Figure S8. HPLC chromatograms for c-di-GMP PDE activities of D289A Mn-TM0186 either (A) as-isolated, (B) as-isolated, pre-incubated with 80 uM ferrous ammonium sulfate (+Fe^{2+}) or (C) as-isolated, pre-incubated with 10 mM manganous chloride (+Mn^{2+}). Samples were withdrawn at the indicated times following addition of c-di-GMP.

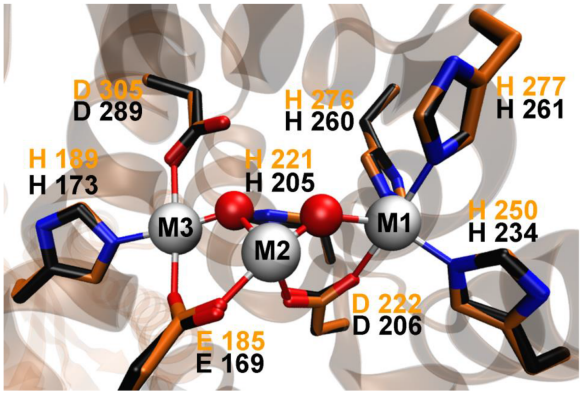

Figure S9. Overlay of the trimetal TM0186 structural model (black) and the PmGH triiron crystal structure (PDB ID 4MCW) (orange).

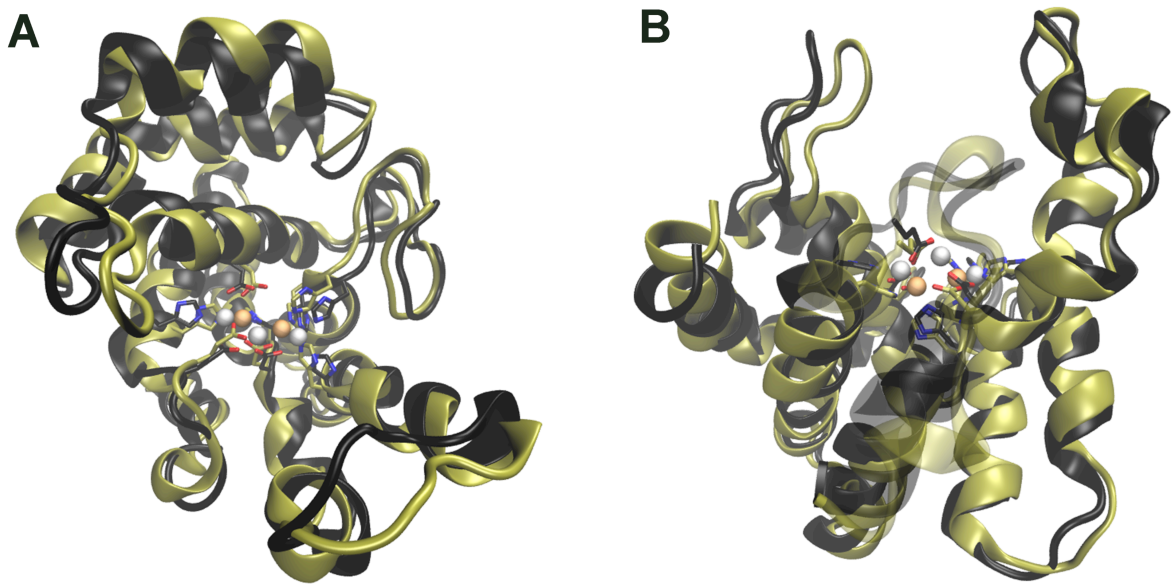

Figure S10. Overlay of the trimetal (black) and dimetal (tan) TM0186 HD-GYP domain backbone structural models from viewed (A) down the substrate channel toward the active site, and (B) ~90 deg rotated from the view in (A) showing the loops lining the substrate channel entry at top. In these views M1 is the right-most metal. Metals are represented as gray spheres for the trimetal model, and gold spheres in the dimetal model. Panel B has residues 155 to 167 transparent for a minimally obstructed view of the metal site.

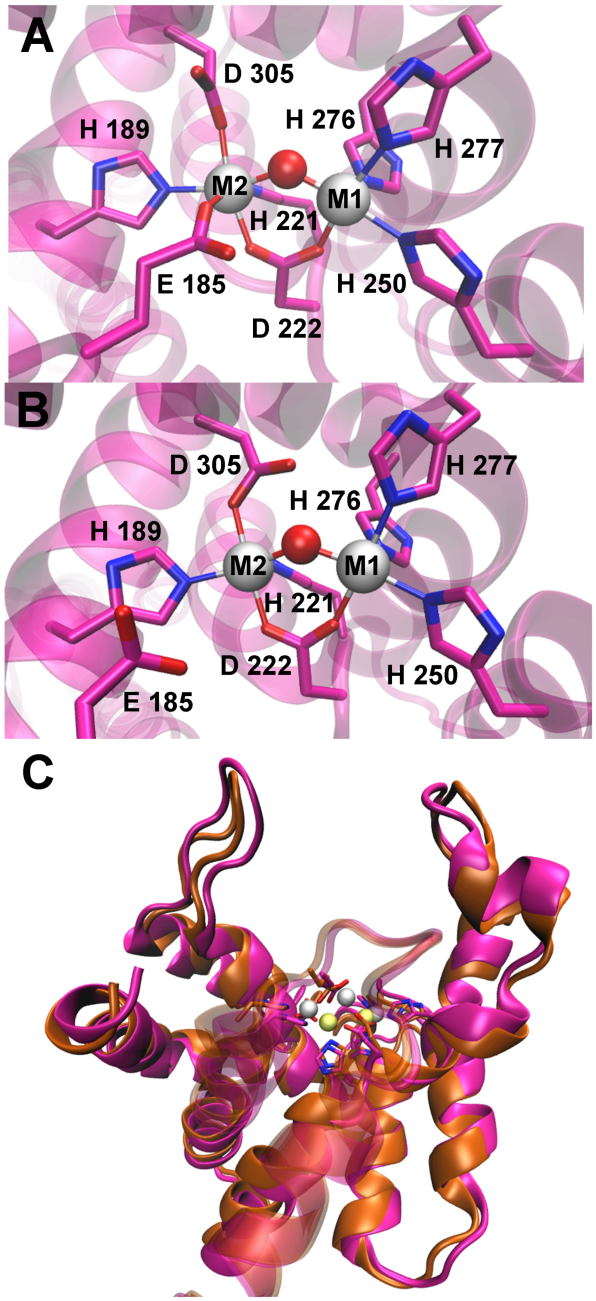

Figure S11. (A) and (B) Views of the dimetal sites in the two subunits of the PmGH dimetal model generated with NAMD using the atom-substituted, solvated PmGH 4MCW coordinates described above as input. (A) Chain A with "E185 on" and (B) chain B with "E185 off". (C) Overlay of the protein backbones of the HD-GYP domains of the trimetal PmGH crystal structure (PDB ID 4MCW) (orange) and dimetal PmGH structural model (magenta) oriented as in Figure S10, Panel B. Panel C has residues 162 to 195 transparent for a minimally obstructed view of the metal site. Lines represent M1-O/N or M2-O,/N interatomic distances within the range of 1.9 - 2.2 Å.

References

(1) Humphrey, W., Dalke, A., and Schulten, K. (1996) VMD: visual molecular dynamics, *J. Mol. Graphics 14*, 33-38, 27-38.

(2) Russell, R. B., and Barton, G. J. (1992) Multiple protein sequence alignment from tertiary structure comparison: assignment of global and residue confidence levels, *Proteins 14*, 309-323.

(3) Phillips, J. C., Braun, R., Wang, W., Gumbart, J., Tajkhorshid, E., Villa, E., Chipot, C., Skeel, R. D., Kale, L., and Schulten, K. (2005) Scalable molecular dynamics with NAMD, *J. Comput. Chem. 26*, 1781-1802.